PMU-Based State Estimation for Networks Containing LCC-HVDC Links

Orestis Darmis, Georgios Karvelis, and George N. Korres, *Senior Member, IEEE*

***Abstract*—This letter proposes an equality-constrained weighted least squares (WLS) state estimation model for networks containing LCC-HVDC links. Voltage and current phasor measurements for the AC network are provided by phasor measurement units (PMUs) and DC voltage and current measurements for the DC transmission lines are acquired by appropriate DC sensors. AC/DC coupling equations and zero injections are treated as equality constraints. Simulation results for a 6-bus hybrid AC/DC network are shown to validate the proposed model and algorithm.**

***Index Terms*—AC/DC state estimation, classic HVDC link, line commutated converter, current source converter, PMU.**

I. Introduction

CONVENTIONAL state estimation (SE) algorithm is performed considering power flow equations [1]. In contrast, PMU-only state estimator utilizes Kirchhoff's laws with voltage and current phasors [2]. The first attempt to include an embedded HVDC link in a SE algorithm, by considering only conventional supervisory control and data acquisition (SCADA) measurements, was in early 80's [3]. In [4], a robust state estimator for interconnected AC and multi-terminal DC (MTDC) transmission systems is proposed, based on the least absolute value (LAV) algorithm. A linear SE for a hybrid AC/DC network, considering only PMU measurements, is presented in [5]. In [6], a PMU-based SE algorithm in polar coordinates is presented, considering classic HVDC links – often referred to as line commutated converters (LCC) or current source converters (CSC) – operating under different control modes. According to the best of the authors' knowledge, a state estimator in rectangular coordinates, including LCC-HVDC links with consideration of all AC/DC coupling equations as equality constraints, has not been reported yet.

The main contributions of the paper are listed as follows:

- AC and DC measurements are modeled independently as functions of AC and DC states, respectively,
- AC and DC measurements (states) are processed (estimated) simultaneously,
- Coupling of AC and DC states is expressed by a set of three nonlinear equality constraints,
- By expressing the state vector in rectangular coordinates, linear PMU measurement equations and linear (nonlinear) equality constraints for zero injections (AC/DC coupling variables) arise. The low nonlinearity leads to faster convergence rate for the SE algorithm to solve as compared with conventional nonlinear SE approaches.

Manuscript received July 29, 2021; revised November 1, 2021 and January 3, 2022; accepted January 12, 2022. Date of publication January 25, 2022; date of current version April 19, 2022. Paper no. PESL-00187-2021. *(Corresponding author: George N. Korres.)*

The authors are with the School of Electrical and Computer Engineering, National Technical University of Athens, 15780 Athens, Greece (e-mail: darmis.orestis@gmail.com; georgios.karvelis@yahoo.com; gkorres@cs.ntua.gr).

Digital Object Identifier 10.1109/TPWRS.2022.3145640

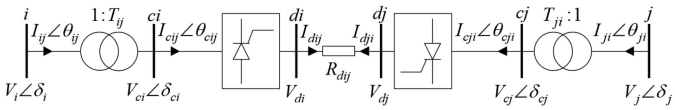

Fig. 1. Single-line diagram of a two-terminal LCC-HVDC transmission link.

II. Model of LCC-HVDC Link

In this section, uppercase (lowercase) notation is used to denote real (per-unit) values of variables. A line commutated converter between AC buses i and j is shown in Fig. 1, where subscript i (j) refers to rectifier (inverter) side of the DC link and virtual AC bus ci (cj) is introduced between transformer and rectifier (inverter).

The equations which relate AC and DC magnitudes between the input and output of the rectifier and inverter are [7]:

$$V_{di} = k_1 N_{ij} T_{ij} V_i \cos(\delta_i - \theta_{ij}) \tag{1a}$$

$$V_{di} = k_1 N_{ij} T_{ij} V_i \cos\alpha_{ij} - k_2 N_{ij} X_{ij} I_{dij} \tag{1b}$$

$$I_{cij} = k_3 N_{ij} I_{dij} \tag{1c}$$

$$V_{dj} = k_1 N_{ji} T_{ji} V_j \cos(\delta_j - \theta_{ji}) \tag{2a}$$

$$V_{dj} = k_1 N_{ji} T_{ji} V_j \cos\gamma_{ji} + k_2 N_{ji} X_{ji} I_{dji} \tag{2b}$$

$$I_{cji} = k_3 N_{ji} I_{dji} \tag{2c}$$

$$I_{dij} = -I_{dji} = (V_{di} - V_{dj})/R_{dij} \tag{3}$$

where T_{ij} (T_{ji}) is the off-nominal turns ratio at the rectifier (inverter) side, X_{ij} (X_{ji}) is the transformer reactance at the rectifier (inverter) side, α_{ij} (γ_{ji}) is the firing (extinction) angle at the rectifier (inverter) side, N_{ij} (N_{ji}) is the number of rectifier (inverter) bridges, $k_1 = 3\sqrt{2}/\pi$, $k_2 = 3/\pi$, and $k_3 = \sqrt{6}/\pi$.

Considering the transformer two-port equations [1], ignoring active power losses, that is $P_{ij} = P_{cij} = P_{dij}$, and expressing all voltage and current phasors in Cartesian form, the following equality constraints can be derived for the rectifier side:

$$0 = -k_1 N_{ij} T_{ij} \sqrt{E_i^2 + F_i^2}\cos\alpha_{ij} + V_{di} + k_2 N_{ij} X_{ij}\left(\frac{V_{di} - V_{dj}}{R_{dij}}\right) \tag{4a}$$

$$0 = \frac{T_{ij}(E_i F_{ci} - F_i E_{ci})}{X_{ij}} + V_{di}\left(\frac{V_{di} - V_{dj}}{R_{dij}}\right) \tag{4b}$$

$$0 = \frac{T_{ij}^2(E_i^2 + F_i^2) + (E_{ci}^2 + F_{ci}^2) - 2T_{ij}(F_i F_{ci} + E_i E_{ci})}{X_{ij}} - 3k_3^2 N_{ij}^2 X_{ij}\left(\frac{V_{di} - V_{dj}}{R_{dij}}\right)^2 \tag{4c}$$

Equality constraints (4a)–(4c) can be transformed into per-unit representation (5a)-(5c) by considering the following base quantities: $Z_{base,i} = V_{base,i}^2/S_{base}$, $Z_{base,ci} = V_{base,ci}^2/S_{base}$, $I_{base,i} = S_{base}/\sqrt{3}V_{base,i}$, $I_{base,ci} = S_{base}/\sqrt{3}V_{base,ci}$ for the AC side and $P_{base} = S_{base}$, $V_{base,di} = V_{base,ci}$, $I_{base,di} = P_{base}/V_{base,di}$, $R_{base,di} = V_{base,di}/I_{base,di} = Z_{base,ci}$ for the DC side.

$$0 = -k_1 N_{ij} t_{ij}\sqrt{e_i^2 + f_i^2}\cos\alpha_{ij} + v_{di} + k_2 N_{ij} x_{ij}\left(\frac{v_{di} - v_{dj}}{r_{dij}}\right) \tag{5a}$$

$$0 = \frac{t_{ij}(e_i f_{ci} - f_i e_{ci})}{x_{ij}} + v_{di}\left(\frac{v_{di} - v_{dj}}{r_{dij}}\right) \tag{5b}$$

$$0 = \frac{t_{ij}^2(e_i^2 + f_i^2) + (e_{ci}^2 + f_{ci}^2) - 2t_{ij}(f_i f_{ci} + e_i e_{ci})}{x_{ij}} - 3k_3^2 N_{ij}^2 x_{ij}\left(\frac{v_{di} - v_{dj}}{r_{dij}}\right)^2 \tag{5c}$$

where t_{ij} is the per-unit off-nominal tap ratio.

Based on (2a)-(2c), equality constraints in per-unit system, similar to (5a)-(5c), can be derived for the inverter side of the HVDC link.

III. Hybrid AC/DC Grid State Estimation

The relationship between the measurement vector z and the state vector x can be expressed as:

$$z = Hx + e \tag{6a}$$

$$0 = c(x) \tag{6b}$$

where H is the constant measurement Jacobian matrix, $c(\cdot)$ is a vector-valued function, and e is the vector of measurement errors, assumed to follow a Gaussian distribution with $\mathrm{cov}(e) = R = diag\{\sigma_1^2, \ldots, \sigma_m^2\}$ and $E(e) = 0$, where σ_i is the standard deviation of the ith measurement.

The state vector x consists of the AC state variables (AC bus voltage phasors expressed in rectangular coordinates) and the DC state variables (DC bus voltages as well as firing and extinction angles). The measurement vector z comprises the AC bus voltage phasors and branch current phasors provided by PMUs as well as the DC voltage and current measurements at the DC transmission lines. The equality constraints include the rectifier and inverter AC/DC coupling equations as well as the zero current injections.

The equality constrained WLS estimator provides the maximum likelihood estimate by repeatedly solving the following system, until $\max|x_{k+1} - x_k|$ is less than a predetermined threshold [1]:

$$\begin{pmatrix} H^T R^{-1} H & C^T(x_k) \\ C(x_k) & 0 \end{pmatrix}\begin{pmatrix} x_{k+1} - x_k \\ \lambda_{k+1} \end{pmatrix} = \begin{pmatrix} H^T R^{-1}(z - Hx_k) \\ -c(x_k) \end{pmatrix} \tag{7}$$

where k is the iteration index, x_k is the solution vector at iteration k, λ_k is the vector of Lagrange multipliers at iteration k, and $C(x_k) = \partial c(x_k)/\partial x$.

A branch $i - j$ (line or transformer) between any two AC buses i and j is represented by the two-port π-model, where $y_{ij} = g_{ij} + jb_{ij} = 1/z_{ij}$ is the series admittance, $z_{ij} = r_{ij} + jx_{ij}$ is the series impedance, and $y_{sij} = g_{sij} + jb_{sij}$ ($y_{sji} = g_{sji} + jb_{sji}$) is the shunt admittance between bus i (j) and the ground. For a line $y_{sij} = y_{sji} = y_{ij0}/2$, where y_{ij0} is the total line shunt admittance. For a transformer, $y_{sij} = t_{ij}(t_{ij} - 1)y_{ij}$ and $y_{sji} = (1 - t_{ij})y_{ij}$, where t_{ij} is the off-nominal p.u. tap ratio at side j. Table I presents AC and DC measurement functions.

It is worth mentioning that the PMU measurement model (6a) is linear and convex, since the AC state variables are written in rectangular form, and only the part of equality constraints (6b) corresponding to HVDC links is nonlinear and nonconvex [8]. As a consequence, the iterative procedure (7) shows improved convergence behavior compared to nonlinear and nonconvex state estimation formulations [8].

All phasor measurements available at different network buses are synchronized with respect to a common synchronizing time signal provided by the global positioning system (GPS) of satellites. Pole-to-ground DC voltage measurements are usually obtained using a resistive-capacitive (RC) voltage divider [9]. For the DC current measurements various current sensor technologies are currently available [9].

The high sampling-rate AC measurements from PMUs and the low sampling-rate DC measurements from HVDC links may not arrive simultaneously at the control center, causing time skewness problem [10]. It is also found that the realistic measurement errors may not follow a Gaussian distribution [11], [12]. To tackle these issues, robust SE approaches are proposed in the literature [10]–[12]. In this study, the DC link measurements are assumed to be sampled synchronously and reported at the same rate as the PMU measurements [5], [6] so that the system of linear equations (7) can be numerically solved at each iteration. It is also assumed that the distribution of the measurement noise is Gaussian.

IV. Simulation Results

The proposed SE algorithm is implemented in MATLAB environment and applied to a 6-bus hybrid AC/DC system with an embedded classic HVDC link between buses 2 and 3, as shown in Fig. 2. The nominal voltage levels of the AC buses are shown in Fig. 2. The impedances of the AC side lines are $j50\,\Omega$ for lines 1-2 and 2-5, $j48\,\Omega$ for line 3-4, and $j32\,\Omega$ for line 3-6. Other network parameters are $N_{23} = N_{32} = 2, T_{23} = 0.18$,

TABLE I
AC AND DC MEASUREMENT FUNCTIONS ($\mathcal{N}_i$ IS THE SET OF AC BUSES ADJACENT TO AC BUS i)

Real and imaginary parts of voltage phasor measurement at bus i	$e_i^{meas} = e_i + e_{e_i}$	$f_i^{meas} = f_i + e_{f_i}$
Real part of current phasor measurement from bus i to bus j	$i_{ij,r}^{meas} = e_i(g_{sij}+g_{ij}) - f_i(b_{sij}+b_{ij}) - e_j g_{ij} + f_j b_{ij} + e_{i_{ij,r}}$	
Imaginary part of current phasor measurement from bus i to bus j	$i_{ij,i}^{meas} = e_i(b_{sij}+b_{ij}) + f_i(g_{sij}+g_{ij}) - e_j b_{ij} - f_j g_{ij} + e_{i_{ij,i}}$	
Real part of zero injected current phasor measurement at bus i	$0 = i_{i,r}^{meas} = e_i \sum_{j\in N_i}(g_{sij}+g_{ij}) - f_i \sum_{j\in N_i}(b_{sij}+b_{ij}) - \sum_{j\in N_i}\left(e_j g_{ij} - f_j b_{ij}\right)$	
Imaginary part of zero injected current phasor measurement at bus i	$0 = i_{i,i}^{meas} = f_i \sum_{j\in N_i}(g_{sij}+g_{ij}) + e_i \sum_{j\in N_i}(b_{sij}+b_{ij}) - \sum_{j\in N_i}(f_j g_{ij} + e_j b_{ij})$	
DC voltage and current measurement at rectifier or inverter side at bus i	$v_{di}^{meas} = v_{di} + e_{v_{di}}$	$i_{dij}^{meas} = (v_{di} - v_{di})/r_{dij} + e_{i_{dij}}$

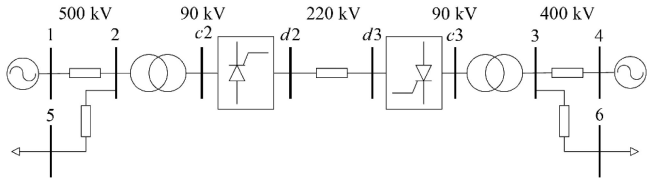

Fig. 2. 6-bus AC/DC system.

TABLE II
DIFFERENT MEASUREMENT SETS FOR THE 6-BUS TEST SYSTEM

Measurement set	PMU measurements	DC measurements
1	z_1	v_{d2}
2	z_1	v_{d2}, v_{d3}
3	z_1	v_{d2}, v_{d3}, i_{d23}
4	z_2	v_{d2}
5	z_2	v_{d2}, v_{d3}
6	z_2	v_{d2}, v_{d3}, i_{d23}

$T_{32} = 0.225$, $X_{23} = X_{32} = 1.377\,\Omega$, and $R_{d23} = 1.13\,\Omega$. The rated capacity of the HVDC link is 350 MW. The virtual buses c_2 and c_3 are considered as zero injection buses. A flat voltage profile ($E_i = 1pu$, $F_i = 0pu$, $v_{di} = 1pu$, $\alpha_{ij} = \gamma_{ij} = 0rad\,\forall i,j$) is chosen for the first iteration of (7) and the tolerance for convergence is set to 10^{-4}.

Gaussian noise is added on the true value of each measurement i as follows:

$$z_i^{meas} = z_i^{true} + rand \times \sigma_i$$

where z_i^{meas} is the measured value, z_i^{true} is the true value obtained from a power flow solution, $rand$ represents a $\mathcal{N}(0,1)$ random number, and standard deviation σ_i is computed as [13]:

$$\sigma_i = \frac{z_i^{true} \times error\%}{3 \times 100}$$

where $error\%$ is a given % of maximum error about z_i^{true}.

For the AC and DC measurements we consider an $error\%$ of 2% and 4%, respectively. Table II shows the AC and DC measurement sets used in the simulations. The measurement vectors z_1 (associated with the PMUs located at buses 2 and 3) and z_2 (associated with the PMUs located at buses 1, 2, 3, and 4) are:

$$z_1 = (e_2\, e_3\, f_2\, f_3\, i_{21,\mathrm{r}}\, i_{23,\mathrm{r}}\, i_{25,\mathrm{r}}\, i_{32,\mathrm{r}}\, i_{34,\mathrm{r}}\, i_{36,\mathrm{r}}\, i_{21,\mathrm{i}}\, i_{23,\mathrm{i}}\, i_{25,i}\, i_{32,\mathrm{i}}\, i_{34,\mathrm{i}}\, i_{36,\mathrm{i}})^T$$

$$z_2 = (e_1\, e_2\, e_3\, e_4\, e_5\, e_6\, f_1\, f_2\, f_3\, f_4\, f_5\, f_6 i_{12,\mathrm{r}}\, i_{21,\mathrm{r}}\, i_{23,\mathrm{r}}\, i_{25,\mathrm{r}}\, i_{52,\mathrm{r}}\, i_{32,\mathrm{r}}\, i_{34,\mathrm{r}}\, i_{43,\mathrm{r}}\, i_{36,\mathrm{r}}\, i_{63,\mathrm{r}}\, i_{12,\mathrm{i}}\, i_{21,\mathrm{i}}\, i_{23,\mathrm{i}}\, i_{25,\mathrm{i}}\, i_{52,\mathrm{i}} i_{32,\mathrm{i}}\, i_{34,\mathrm{i}}\, i_{43,\mathrm{i}}\, i_{36,\mathrm{i}}\, i_{63,\mathrm{i}})^T$$

Study cases with error-free measurements and corrupted measurements with gross errors are considered.

A. Test Cases Without Bad Data

In this subsection all measurements are assumed exact. The estimated states for the different cases are given in Table III. As evident from this table, the difference between estimated and true states is negligible. The maximum absolute differences of AC states are 2×10^{-4} p.u. for voltages (cases 1, 2, and 3, v_6) and 3.7×10^{-3} degrees for angles (case 3, δ_6). The maximum absolute differences of DC states are 1×10^{-4} p.u. for voltages (case 4, v_{d3}) and 4×10^{-2} degrees for angles (case 1, γ_{23}). In all test cases convergence is achieved in 2 iterations.

B. Test Cases With Bad Data

In this subsection two cases with bad data are studied. The largest normalized residual test processes successive cycles of estimation and reestimation with suspect measurements being eliminated from the measurement set until all normalized residuals are below a predefined threshold (usually chosen as 3, which corresponds to approximately 0.1% probability of false alarm), signaling that no more bad data are present. We consider the measurement set 6 of Table III and two cases of gross errors:

- 20σ and -15σ on current and voltage measurements $i_{12,r}$ and v_{d2} ,
- 15σ and -20σ on voltage measurements e_1 and v_{d3}.

The two largest normalized residuals of each estimation-reestimation cycle are shown in Table IV. The measurement with the highest normalized residual is eliminated at the end of each cycle and the state is reestimated. After two reestimation steps, the erroneous measurements are correctly flagged as bad data.

TABLE III
STATE ESTIMATION RESULTS FOR THE 6-BUS TEST SYSTEM

State Variable	Power Flow Results	Case 1	Case 2	Case 3	Case 4	Case 5	Case 6
$\tilde{v}_1$	$1.02\angle 0^\circ$	$1.0199\angle 0.002^\circ$	$1.0199\angle 0.003^\circ$	$1.0199\angle 0.003^\circ$	$1.02\angle 0.001^\circ$	$1.02\angle 0.001^\circ$	$1.02\angle 0.001^\circ$
$\tilde{v}_2$	$0.9774\angle -5.213^\circ$	$0.9773\angle -5.211^\circ$	$0.9773\angle -5.211^\circ$	$0.9773\angle -5.211^\circ$	$0.9773\angle -5.212^\circ$	$0.9773\angle -5.212^\circ$	$0.9773\angle -5.212^\circ$
$\tilde{v}_3$	$0.9743\angle 4.287^\circ$	$0.9741\angle 4.284^\circ$	$0.9741\angle 4.284^\circ$	$0.9741\angle 4.284^\circ$	$0.9742\angle 4.285^\circ$	$0.9742\angle 4.285^\circ$	$0.9742\angle 4.285^\circ$
$\tilde{v}_4$	$1.03\angle 0^\circ$	$1.0299\angle -0.003^\circ$	$1.0299\angle -0.003^\circ$	$1.0299\angle -0.003^\circ$	$1.0299\angle -0.001^\circ$	$1.0299\angle -0.001^\circ$	$1.0299\angle -0.001^\circ$
$\tilde{v}_5$	$0.9668\angle -6.426^\circ$	$0.9667\angle -6.424^\circ$	$0.9667\angle -6.424^\circ$	$0.9667\angle -6.424^\circ$	$0.9668\angle -6.425^\circ$	$0.9668\angle -6.425^\circ$	$0.9668\angle -6.425^\circ$
$\tilde{v}_6$	$0.9637\angle 3.066^\circ$	$0.9635\angle 3.063^\circ$	$0.9635\angle 3.063^\circ$	$0.9635\angle 3.062^\circ$	$0.9636\angle 3.065^\circ$	$0.9636\angle 3.065^\circ$	$0.9636\angle 3.065^\circ$
$\tilde{v}_{c2}$	$0.9558\angle -8.895^\circ$	$0.9557\angle -8.892^\circ$	$0.9557\angle -8.892^\circ$	$0.9557\angle -8.892^\circ$	$0.9558\angle -8.893^\circ$	$0.9558\angle -8.893^\circ$	$0.9558\angle -8.893^\circ$
$\tilde{v}_{c3}$	$0.9373\angle 8.093^\circ$	$0.9371\angle 8.090^\circ$	$0.9371\angle 8.090^\circ$	$0.9371\angle 8.090^\circ$	$0.9371\angle 8.091^\circ$	$0.9371\angle 8.091^\circ$	$0.9371\angle 8.091^\circ$
v_{d2}	1.0082	1.0082	1.0082	1.0082	1.0082	1.0082	1.0082
v_{d3}	1.00	1.00	1.00	1.00	1.0001	1.00	1.00
α_{23}	17.98°	17.957°	17.960°	17.960°	17.966°	17.969°	17.969°
γ_{23}	15.35°	15.309°	15.3121°	15.3121°	15.324°	15.329°	15.329°

TABLE IV
NORMALIZED RESIDUAL TESTS FOR BAD DATA IDENTIFICATION

Cycle	1		2		3	
Meas.	$i_{12,r}$	v_{d2}	v_{d2}	v_{d3}	v_{d3}	f_1
$\lvert r_{N,\max}\rvert$	15.854	15.332	13.476	8.979	2.843	2.093
Meas.	v_{d3}	e_1	e_1	$i_{23,i}$	$i_{23,i}$	v_{d2}
$\lvert r_{N,\max}\rvert$	22.665	15.568	12.590	4.016	0.340	0.313

V. CONCLUSION

In this paper a PMU-based state estimator for power systems with embedded classic HVDC links has been introduced. All the AC and DC state variables are simultaneously considered to solve an equality constrained WLS problem, using PMU measurements from the AC network and DC measurements from the DC links. In future work, we will develop a hybrid SCADA/PMU estimator for AC/DC power systems and will investigate the impacts of non-Gaussian measurement error and measurement imperfect synchronization and skewness on state estimation process.

REFERENCES

[1] A. Abur and A. G. Expósito, *Power System State Estimation: Theory and Implementation*. New York, NY, USA: Marcel Dekker, 2004.

[2] A. G. Phadke, J. S. Thorp, and K. J. Karimi, "State estimation with phasor measurements," *IEEE Trans. Power Syst.*, vol. 1, no. 1, pp. 233–238, Feb. 1986.

[3] H. R. Sirisena and E. P. M. Brown, "Inclusion of HVDC links in AC power-system state estimation," *IEE Proc. C-Generat. Transmiss. Distrib.*, vol. 128, no. 3, pp. 147–154, May 1981.

[4] A. Mouco and A. Abur, "A robust state estimator for power systems with HVDC components," in *Proc. North Amer. Power Symp.*, Sep. 2017, pp. 1–5.

[5] W. Li and L. Vanfretti, "Inclusion of classic HVDC links in a PMU-based state estimator," in *Proc. IEEE PES Gen. Meeting*, Jul. 2014, pp. 1–5.

[6] W. Li and L. Vanfretti, "A PMU-based state estimator considering classic HVDC links under different control modes," *Sustain. Energy, Grids Netw.*, vol. 2, pp. 69–82, Jun. 2015.

[7] E. W. Kimbark, *Direct Current Transmission*, vol. I. New York, NY, USA: Wiley, 1971.

[8] S. Boyd and L. Vandenberghe, *Convex Optimization*. Cambridge, U.K.: Cambridge Univ. Press, 2006.

[9] D. Tzelepis *et al.*, "Voltage and current measuring technologies for high voltage direct current supergrids: A technology review identifying the options for protection, fault location and automation applications," *IEEE Access*, vol. 8, pp. 203398–203428, 2020.

[10] J. Zhao, S. Wang, L. Mili, B. Amidan, R. Huang, and Z. Huang, "A robust state estimation framework considering measurement correlations and imperfect synchronization," *IEEE Trans. Power Syst.*, vol. 33, no. 4, pp. 4604–4613, Jul. 2018.

[11] J. Zhao and L. Mili, "A framework for robust hybrid state estimation with unknown measurement noise statistics," *IEEE Trans. Ind. Informat.*, vol. 14, no. 5, pp. 1866–1875, May 2018.

[12] T. Chen, L. Sun, K. Ling, and W. Ho, "Robust power system state estimation using t-distribution noise model," *IEEE Syst. J.*, vol. 14, no. 1, pp. 771–781, Mar. 2020.

[13] G. N. Korres and N. M. Manousakis, "State estimation and bad data processing for systems including PMU and SCADA measurements," *Electric Power Syst. Res.*, vol. 81, no. 7, pp. 1514–1524, Jul. 2011.